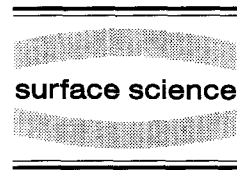




ELSEVIER

Surface Science 324 (1995) 345–356



Methane activation and dehydrogenation on nickel and cobalt: a computational study

H. Burghraef^{*}, A.P.J. Jansen, R.A. van Santen

*Laboratory for Inorganic Chemistry and Catalysis / Theory Group, Eindhoven University of Technology, P.O. Box 513,
5600 MB Eindhoven, Netherlands*

Received 18 August 1994; accepted for publication 19 October 1994

Abstract

We have studied the adsorption of CH_3 and H on nickel clusters of various size and shape. As a next step we have chosen a one-layer 7-atom cluster and a spherical 13-atom cluster to model the nickel and cobalt surface and we have studied the adsorption of CH_3 , CH_2 , CH, C, and H on these clusters. Starting from gas phase CH_4 , the formation of adsorbed CH_3 (CH_{3a}) and adsorbed H (H_a) is endothermic on all clusters, but the endothermicity is strongly reduced on the 13-atom clusters (142 kJ/mol on Ni_7 , 135 kJ/mol on Co_7 , 30 kJ/mol on Ni_{13} , and 8 kJ/mol on Co_{13}). The formation of adsorbed CH_2 (CH_{2a}) and H_a from CH_{3a} is endothermic by 25–40 kJ/mol on all clusters, except on Co_7 (3 kJ/mol exothermic), mainly because of the much stronger adsorption of CH_2 on this cluster. The formation of adsorbed CH (CH_a) and H_a from CH_{2a} is exothermic on all clusters, but the exothermicity differs a factor two between the 7- and 13-atom clusters (61 kJ/mol on Ni_7 , 60 kJ/mol on Co_7 , 27 kJ/mol on Ni_{13} , and 32 kJ/mol on Co_{13}). Finally, the formation of adsorbed C (C_a) and H_a from CH_a is strongly endothermic on the 7-atom clusters, but the endothermicity is again strongly reduced on the 13-atom clusters (92 kJ/mol on Ni_7 , 77 kJ/mol on Co_7 , 27 kJ/mol on Ni_{13} , and 14 kJ/mol on Co_{13}).

Keywords: Chemisorption; Clusters; Density functional calculations

1. Introduction

One of the most important catalytic reactions on surfaces is the reforming of CH_4 producing higher hydrocarbons. Various carbonaceous species have been proposed to be intermediates during this reaction, but the exact nature of these intermediates is still under discussion. The group of Ceyer [1] reported the existence of CH_3 and CH on a Ni(111) surface using HREELS. Kaminsky et al. [2] observed

all CH_x fragments on Ni(111) using SIMS, and according to them the stability of carbon, methyldyne, methylene, and methyl is similar. In this study we will discuss the energetics, adsorbate–substrate distance, and frequency of all possible single carbon CH_x species and H on cobalt and nickel, which have been modelled by various cluster models. First, we will investigate the advantages and disadvantages of the different cluster models by means of the chemisorption behaviour of CH_3 and H, followed by the study of methane dissociation and subsequent dehydrogenation of the CH_x species on our best cluster models, which are a one-layer 7-atom cluster and a spherical 13-atom cluster. Thus, we have

^{*} Corresponding author.

studied the following reactions on nickel and cobalt clusters:



For reaction (1) $\text{M} = \text{Ni}$ or Co , and $x = 7$ or 13 .

Details of the calculations are discussed in Section 2. In Section 3.1 we present and discuss CH_3 and H adsorption on various nickel clusters. In Section 3.2 we discuss the chemisorption of the other CH_x species on Ni_7 and Ni_{13} . In Section 3.3 the chemisorption of H and all CH_x species on Co_7 and Co_{13} is discussed. In Section 4 we summarize results and draw some conclusions.

2. Methods

We have carried out quasi-relativistic calculations based on density functional theory (DFT) using the Amsterdam density functional program package (ADF) developed by Baerends et al. [3]. The exchange–correlation potential used is based on quantum Monte Carlo simulations of Ceperley and Alder [4] of a homogeneous electron gas which are parametrized by Vosko, Wilk and Nusair [5]. To correct for the overbinding inherent to the local density approximation (LDA) [6], we have used a gradient corrected exchange energy functional [7] in combination with the Stoll correction [8] for correlation. For carbon a frozen core potential is used for the 1s electrons; for nickel and cobalt the electrons up to 3p are frozen. Relativistic effects were taken

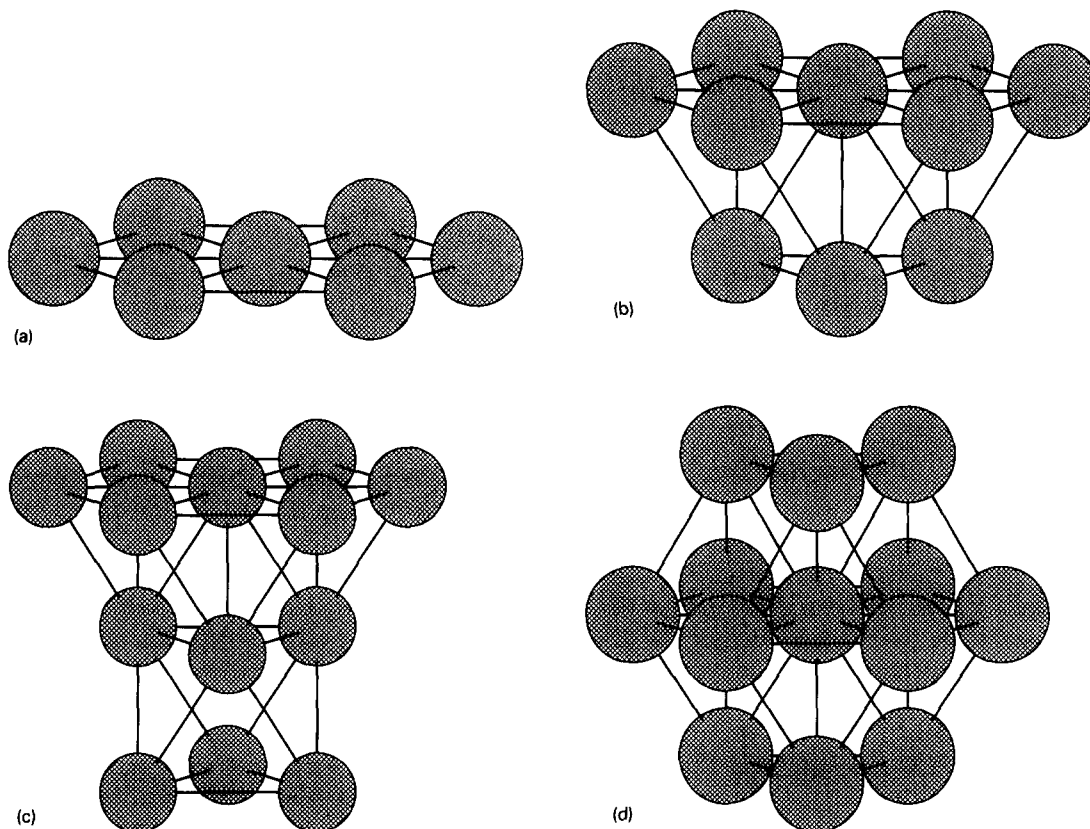


Fig. 1. Different clusters modeling the substrate. (a) Ni_7 cluster, (b) $\text{Ni}_{7,3}$ cluster, (c) $\text{Ni}_{7,3,3}$ cluster, (d) Ni_{13} cluster. For all clusters the bond distance of the bulk was used (2.49 Å for Ni, 2.50 Å for Co).

into account by first-order perturbation theory [9]. s- and p-orbitals are of double ζ quality, d orbitals of triple ζ quality. On all atoms polarization functions are included. Rösch et al. [10] and Kühnholz et al. [11] have shown that clusters can model substrate surfaces and the bulk metal within DFT. Therefore, we have used Ni, Ni₇, Ni_{7,3}, Ni_{7,3,3}, and Ni₁₃ clusters as substrate models for nickel. This last cluster does not model a specific crystal plane, but consists of a central nickel atom surrounded by 12 atoms in a hexagonal closed-packed fashion for reasons of symmetry. In this cluster, all surface nickel atoms form bonds with five other nickel atoms and there are no low coordinated boundary atoms, eliminating possible boundary effects. For all nickel clusters the bond distance was fixed at the bulk value of 2.49 Å. The various substrate models are shown in Figs. 1a–1d. For cobalt we modelled the substrate using the one-layer 7-atom cluster and the 13-atom cluster described above. The cobalt bond distance was fixed at 2.50 Å, which is the bulk value.

Adsorption energies are calculated using Ziegler's transition state method [12] and are given relative to the gas phase fragments with the same geometry. These are the following. For all CH_x species we kept the CH distances at 1.08 Å. For CH₃ the HCH angles are 109.48° as are the substrate CH angles. For CH₂ the HCH angle is 109.48° and the substrate CH angles are 125.26°. For CH the substrate CH angles are 180°. The electronic states with respect to which the adsorption energies of the species are given are for C the ³P state, for CH the ²Π state, for CH₂ the ¹A₁ state and for CH₃ the ²A₁ state. We have also evaluated the energy difference between CH₂ (¹A₁) and CH₂ (³Σ_g), and between CH₃ (²A₁) and CH₃ (²A₂), which are the experimental ground states.

3. Results and discussion

3.1. CH₃ and H adsorption on nickel clusters

To find a suitable model for the substrate, we have studied the chemisorption of CH₃ and H on various nickel clusters. The results are shown in Table 1. CH₃ clearly prefers the one-fold site on

Table 1
CH₃ and H chemisorption data on various nickel clusters

Adsorbate	Substrate	Site	<i>z</i> (Å)	<i>E</i> _{ads} (kJ/mol)	<i>ν</i> (cm ⁻¹)
CH ₃ ^a	Ni	1-fold	1.97	296	447
CH ₃	Ni ₇	1-fold	2.06	97	387
CH ₃	Ni ₇	2-fold	1.92	61	245
CH ₃	Ni ₇	3-fold	1.96	64	307
CH ₃	Ni _{7,3}	1-fold	2.02	113	231
CH ₃	Ni _{7,3}	2-fold	2.03	86	308
CH ₃	Ni _{7,3}	3-fold	2.06	76	310
CH ₃	Ni _{7,3,3}	1-fold	2.09	109	324
CH ₃	Ni _{7,3,3}	2-fold	1.98	94	491
CH ₃	Ni _{7,3,3}	3-fold	1.88	83	550
CH ₃	Ni ₁₃	1-fold	1.99	179	465
CH ₃	Ni ₁₃	2-fold	1.87	152	292
CH ₃	Ni ₁₃	3-fold	1.90	143	271
H	Ni	1-fold	1.50	304	1976
H	Ni ₇	1-fold	1.48	203	1913
H	Ni ₇	2-fold	1.04	229	1472
H	Ni ₇	3-fold	0.90	241	1014
H	Ni _{7,3}	1-fold	1.53	224	1951
H	Ni _{7,3}	2-fold	1.10	218	1670
H	Ni _{7,3}	3-fold	0.95	253	1724
H	Ni _{7,3,3}	1-fold	1.48	212	1703
H	Ni _{7,3,3}	2-fold	1.12	231	1774
H	Ni _{7,3,3}	3-fold	0.87	242	2118
H	Ni ₁₃	1-fold	1.51	235	1764
H	Ni ₁₃	2-fold	1.13	253	1119
H	Ni ₁₃	3-fold	1.14	272	1284

Adsorption energies are given relative to the gas phase fragments with the same geometry in their lowest electronic state. For more specific details, see Section 2. *z* denotes the perpendicular adsorbate–substrate distance, *ν* denotes the adsorbate–substrate vibrational stretch frequency.

^a All CH₃ adsorption energies drop 34 kJ/mol if we allow for CH₃ relaxation in the gas phase to adopt the preferred planar CH₃ (²A₂) configuration.

Ni₇, followed by the three-fold site and the two-fold site. The adsorption energies of respectively 97, 64 and 61 kJ/mol are far lower than values calculated by others. If we allow for relaxation of CH₃ in the gas phase to adopt the preferred planar geometry, all adsorption energies decrease by 34 kJ/mol. Extending our cluster model by adding a second layer of 3 atoms enlarges the adsorption energy with 12–25 kJ/mol. Adding another third layer of 3 atoms enlarges the energy with 12–33 kJ/mol with respect to the Ni₇ cluster. Comparing the Ni_{7,3} and Ni_{7,3,3} clusters, the two-fold and three-fold positions are

favoured another 8 kJ/mol, but the one-fold site shifts 4 kJ/mol downwards. This is an example of the oscillation of adsorption energy with cluster size and/or shape, although the effect is relatively small. Using the Ni₁₃ cluster, the adsorption energy increases significantly for all sites with an approximately equal amount (79–91 kJ/mol) with respect to the Ni₇ cluster, resulting in energies of 179 kJ/mol for the one-fold site, 152 kJ/mol for the two-fold site, and 143 kJ/mol for the three-fold site. Resuming the site preference, on all clusters the one-fold position is clearly preferred, followed by the two-fold and three-fold positions, whose adsorption energies are closer to each other than to the one-fold chemisorption energy. The only exception is the Ni cluster where the two- and three-fold site have almost the same energy with a slight preference for the three-fold site. For the most preferred site on Ni₇, the one-fold site, we have also optimized the adsorption energy as a function of CH bond distance, adsorbate–substrate distance and HCH angle simultaneously. It turned out that in the optimal geometry the CH bonds had increased (from 1.08 to 1.11 Å), the adsorbate–substrate distance shortened (from 2.06 to 1.95 Å), and the substrate CH angles increased (from 109.48° to 112.15°). However, the adsorption energy with respect to the CH₃ fragment in the same geometry in the gas phase increases only marginal with 3 kJ/mol. We therefore conclude that relaxation of the adsorbate affects the adsorption energy very little. The ability to move along the surface (mobility) is in our model inversely proportional to the difference in adsorption energy between the most preferred site and the next-most preferred site. The energy difference between the sites can be interpreted as the barrier which has to be overcome to move along the surface, where we have implicitly assumed that there is no intermediate geometry with a worse adsorption energy than the next-most preferred site. Therefore, the higher this barrier the lower the mobility. This mobility barrier is 33 kJ/mol for the Ni₇ cluster, 27 kJ/mol for the Ni_{7,3} cluster, 15 kJ/mol for the Ni_{7,3,3} cluster, and 27 kJ/mol for the Ni₁₃ cluster, indicating that CH₃ is quite mobile on all these clusters. Adsorbate–substrate distances range between 1.99–2.10 Å for the one-fold sites, 1.87–2.03 Å for the two-fold sites, and 1.87–2.06 Å for the three-fold sites. The adsorbate–substrate

stretch frequency varies strongly among the sites and among the clusters on first sight, but on closer inspection the one-fold site frequency has a much lower value than the two-fold sites and three-fold site frequency on the Ni_{7,3} and Ni_{7,3,3} clusters. We attribute this effect to the oscillation of frequencies on cluster size and/or shape equivalently to the well known oscillation of adsorption energy on cluster size and/or shape. On the Ni₇ and Ni₁₃ clusters, this trend is just the opposite and more in line with our expectation.

Siegbahn et al. [13] performed MRCCI calculations and used so-called bond prepared clusters. For CH₃ adsorption on Ni(111) modelled by a Ni₃ cluster, a value of 174 kJ/mol was calculated. Using the same cluster with the more extended basis and more reference states, they found a value of 205 kJ/mol for the high coordinated positions. In a previous study [14] on Ni(111) now modelled by a Ni_{3,1}, Ni_{3,7,7,3}, and a Ni_{12,7,3} cluster, they concluded on the basis of energies and frequencies that CH₃ adsorbs at a three-fold site. They calculated the adsorption energy for this site in the range 188–209 kJ/mol and estimated it to be in the range 209–230 kJ/mol. For the one-fold site modelled by a single atom and a Ni_{7,3} cluster, their estimate was 180–201 kJ/mol.

Yang and Whitten [15] performed ab initio valence orbital CI calculations and used an embedded cluster modelling a Ni(111) surface. They calculated for the one-fold position of CH₃ an adsorption energy of 142 kJ/mol, a surface–CH₃ distance of 2.03 Å, and a surface–CH₃ stretch frequency of 416 cm⁻¹. For the two-fold position, they found an energy of 149 kJ/mol, a surface–CH₃ distance of 1.98 Å, and a surface–CH₃ frequency of 296 cm⁻¹. Finally, for the three-fold position an adsorption energy of 162 kJ/mol, a surface–CH₃ distance of 1.83 Å, and a surface–CH₃ frequency of 369 cm⁻¹ was calculated.

The only experimental data on CH₃ adsorption on Ni(111) is the surface–CH₃ stretch frequency, which is 370 cm⁻¹ [1]. On the basis of this frequency our best model for a Ni(111) surface, which is the Ni_{7,3,3} cluster, suggests adsorption at the one-fold site, as does the Ni cluster. Therefore, both frequency and adsorption energy point to adsorption at the one-fold site. Also on the Ni₁₃ cluster the one-fold position is clearly preferred. It is clear that our results differ

significantly from those of Siegbahn and Yang and Whitten. They agree on the preferred adsorption site, which is according to them three-fold, but their computation of the adsorption energy differs 47–68 kJ/mol, if we use Siegbahn's best estimate. Although Siegbahn used bond prepared clusters the adsorption energy still varies significantly between the different clusters. Furthermore, Schüle et al. [14] expect the one-fold vibrational frequency to be around 600 cm^{-1} based on their single atom model, whereas Yang and Whitten give for this frequency a value of 416 cm^{-1} . If we compare our single atom data with our one-fold Ni_7 cluster (Table 1), it shows that in the single atom case the adsorption energy and vibrational frequency are much higher, suggesting that it is not straightforward to compare a single nickel atom with a $\text{Ni}(111)$ surface. On our Ni_7 cluster we calculate the highest stretch frequency for the one-fold position, followed by the three-fold and two-fold site. Yang and Whitten find the same order, but all their frequencies are $30\text{--}60\text{ cm}^{-1}$ higher.

If we compare the experimental surface- CH_3 stretch frequency with our computed results, the one-fold site on the Ni_7 cluster seems the best model for CH_3 adsorption. Adsorption at the various sites on $\text{Ni}_{7,3}$ and $\text{Ni}_{7,3,3}$ clusters results in more or less the same adsorption energy, but the adsorbate-substrate stretch frequencies at the one-fold site are significantly below those on the two-fold and three-fold sites, which runs contrary to chemical intuition and is also in disagreement with the computed frequencies of Yang and Whitten. Their adsorbate-substrate stretch frequencies are always highest on one-fold sites. The Ni_7 , $\text{Ni}_{7,3}$, and $\text{Ni}_{7,3,3}$ cluster models have all as their main disadvantage a strongly endothermic dissociation of CH_4 (reaction 1), whereas it should be more or less thermoneutral. This is remedied by choosing the Ni_{13} cluster as our substrate model. In this model, all twelve surface atoms are equally unsaturated with bonds, i.e. five bonds instead of the bulk value of twelve, and therefore it forms a relatively strong bond with any adsorbate. In this cluster boundary effects cannot occur, contrary to all other substrate models.

For H adsorption on the Ni_7 cluster, we calculated a preference for the three-fold site, with a surface-H distance of 0.90 \AA , an adsorption energy

of 241 kJ/mol and a surface-H frequency of 1014 cm^{-1} . Adding a second layer affects the adsorption sites very differently, destabilizing the two-fold site by 10 kJ/mol and stabilizing the one-fold site by 22 kJ/mol . For the $\text{Ni}_{7,3,3}$ cluster the adsorption energies strongly resemble those on the Ni_7 cluster. The largest difference is for the one-fold site which is stabilized now by 10 kJ/mol . For the Ni_{13} cluster the adsorption energies are shifted more or less the same by $24\text{--}32\text{ kJ/mol}$, resulting in a favoured three-fold site with adsorption energy of 272 kJ/mol . The barrier to move along the surface is 13 kJ/mol on the Ni_7 cluster, 29 kJ/mol on the $\text{Ni}_{7,3}$ cluster, 11 kJ/mol on the $\text{Ni}_{7,3,3}$ cluster, and 19 kJ/mol on the Ni_{13} cluster. Again the stretch frequencies vary strongly between the different cluster models, but the value for the three-fold site on the Ni_7 cluster is quite close to the experimental value. The three-fold site frequencies on the $\text{Ni}_{7,3}$ and $\text{Ni}_{7,3,3}$ clusters seem too high, and in the case of the $\text{Ni}_{7,3,3}$ cluster it is again higher than the one-fold site frequency. Panas et al. [16] studied high coordinated adsorption of hydrogen using many clusters modelling $\text{Ni}(111)$ surfaces. Averaging over the different cluster models, they found a value of 258 kJ/mol for clusters modelling the $\text{Ni}(111)$ surface. No data on frequencies or adsorbate-substrate distances was given. Yang and Whitten [13] found for hydrogen a preference for the three-fold site, with an adsorption energy of 259 kJ/mol , a surface-H distance of 1.16 \AA , and a surface-H frequency of 1043 cm^{-1} , which is in good agreement with our results on Ni_7 . For the two-fold site they found an adsorption energy of 248 kJ/mol , a surface-H distance of 1.31 \AA and a surface-H frequency of 1183 cm^{-1} . For the one-fold site they computed an adsorption energy of 187 kJ/mol , a surface-H distance of 1.61 \AA and a surface-H frequency of 2332 cm^{-1} . Except for the one-fold adsorption energy, this is also in good agreement with our results quantitatively. For hydrogen adsorption on $\text{Ni}(111)$ more experimental data is available. The experimental site preference for H is three-fold with a surface-H distance of 1.15 \AA [17], an adsorption energy of 261 kJ/mol [18], and a surface-H frequency of 1120 cm^{-1} [19].

We conclude that there is good agreement between our results and those of Siegbahn et al. and Yang and Whitten with respect to hydrogen adsorp-

tion. All groups produce adsorption energies, surface–H distances and surface–H frequencies, which compare well with the available experimental data. On the other hand, the computed CH₃ chemisorption data differ significantly between the groups, while experimental data is scarce. A possible origin of these differences is the treatment of the nickel d orbitals. Yang and Whitten include for their local surface region of four nickel atoms the valence d orbitals. All other nickel atoms are described by an effective core potential (ECP). Also, the inclusion of two more nickel atoms in the second layer of their cluster favours now hydrogen adsorption at the hollow (fcc) site by 2 kJ/mol, whereas without these two nickel atoms the filled (hcp) site is favoured by 15 kJ/mol, indicating the susceptibility of their cluster choice. Siegbahn et al. described all nickel atoms modelling hollow (three-fold) sites by ECPs. For on top bonding, the directly bonding metal atom was described at the all electron level. In all cases effects of 3d correlation have not been included. In the case of oxygen adsorbed at the four-fold hollow site of Cu(100), this correlation effect turned out to be 55 kJ/mol. Rösch et al. [10] have shown in a DFT study on small to medium sized clusters that the 3d manifold is narrow and the bonding in the cluster is largely due to 4s/4p-type electrons. Therefore the highly localized 3d orbitals are not expected to contribute directly to the bonding in the clusters and other groups [20] suggested that they thus could be described by ECPs. However, it is known that 3d orbitals are directly involved in a large number of chemisorption bonds and they at least provide an efficient way to rehybridize and to reduce the Pauli repulsion with the adsorbed molecule, which is important in the formation of a chemical bond. Our method of explicitly treating the valence d orbitals on all nickel atoms seems in this light a more reliable method. More experimental or computational data based on different methodologies is therefore very interesting and necessary to draw more conclusions on CH₃ adsorption. Both Ni₇ and Ni₁₃ seem appropriate models. Especially the three-fold adsorbate–substrate stretch frequency on the Ni_{7,3} and Ni_{7,3,3} clusters are too high. On the basis of both CH₃ and H adsorption on the various cluster models, the Ni₇ and Ni₁₃ clusters seem the most suitable substrate models.

3.2. CH₂, CH, and C adsorption on nickel clusters

To study the decomposition of CH_{3a} to CH_{2a}, CH_a and eventually C_a on nickel and cobalt, we have used the 7-atom cluster and the 13-atom cluster. In this section we will discuss the results for nickel,

Table 2
CH₃, CH₂, CH, C, and H chemisorption data on Ni₇, and Ni₁₃ clusters

Adsorbate	Substrate	Site	<i>z</i> (Å)	<i>E</i> _{ads} (kJ/mol)	<i>ν</i> (cm ⁻¹)
CH ₃ ^a	Ni ₇	1-fold	2.06	97	387
CH ₃	Ni ₇	2-fold	1.92	61	245
CH ₃	Ni ₇	3-fold	1.96	64	307
CH ₃	Ni ₁₃	1-fold	1.99	179	465
CH ₃	Ni ₁₃	2-fold	1.87	152	292
CH ₃	Ni ₁₃	3-fold	1.90	143	271
CH ₂ ^b	Ni ₇	1-fold	1.81	225	535
CH ₂	Ni ₇	2-fold	1.60	263	439
CH ₂	Ni ₇	3-fold	1.44	312	496
CH ₂	Ni ₁₃	1-fold	1.81	301	565
CH ₂	Ni ₁₃	2-fold	1.49	285	464
CH ₂	Ni ₁₃	3-fold	1.45	378	592
CH	Ni ₇	1-fold	1.66	245	538
CH	Ni ₇	2-fold	1.27	488	700
CH	Ni ₇	3-fold	1.14	536	730
CH	Ni ₁₃	1-fold	1.70	347	771
CH	Ni ₁₃	2-fold	1.35	437	555
CH	Ni ₁₃	3-fold	1.25	537	594
C	Ni ₇	1-fold	1.66	359	705
C	Ni ₇	2-fold	1.27	505	566
C	Ni ₇	3-fold	1.14	559	742
C	Ni ₁₃	1-fold	1.66	378	701
C	Ni ₁₃	2-fold	1.26	476	551
C	Ni ₁₃	3-fold	1.08	595	551
H	Ni ₇	1-fold	1.48	203	1913
H	Ni ₇	2-fold	1.04	229	1472
H	Ni ₇	3-fold	0.90	241	1014
H	Ni ₁₃	1-fold	1.51	235	1764
H	Ni ₁₃	2-fold	1.13	253	1119
H	Ni ₁₃	3-fold	1.12	272	1284

Adsorption energies are given relative to the gas phase fragments with the same geometry in their lowest electronic state. For more specific details, see Section 2. *z* denotes the perpendicular adsorbate–substrate distance, *ν* denotes the adsorbate–substrate vibrational stretch frequency.

^a All CH₃ adsorption energies drop 34 kJ/mol if we allow for CH₃ relaxation in the gas phase to adopt the preferred planar CH₃ (²A₂⁺) configuration.

^b All CH₂ adsorption energies drop 25 kJ/mol if we allow for CH₂ relaxation in the gas phase to adopt the preferred CH₂ (³Σ_g⁻) configuration.

which are displayed in Table 2 and Fig. 2a,2b. For completeness, we have also added the CH_3 and H chemisorption data on these clusters. CH_2 prefers the three-fold site on both clusters with a chemisorption energy of 312 kJ/mol on Ni_7 and 378 kJ/mol

on Ni_{13} . To allow for CH_2 relaxation in the gas phase, we have to shift the adsorption energies of CH_2 with 25 kJ/mol downward. This is the energy difference between CH_2 ($^1\text{A}_1$), which is the reference in our tables, and CH_2 ($^3\Sigma_g$), which is the

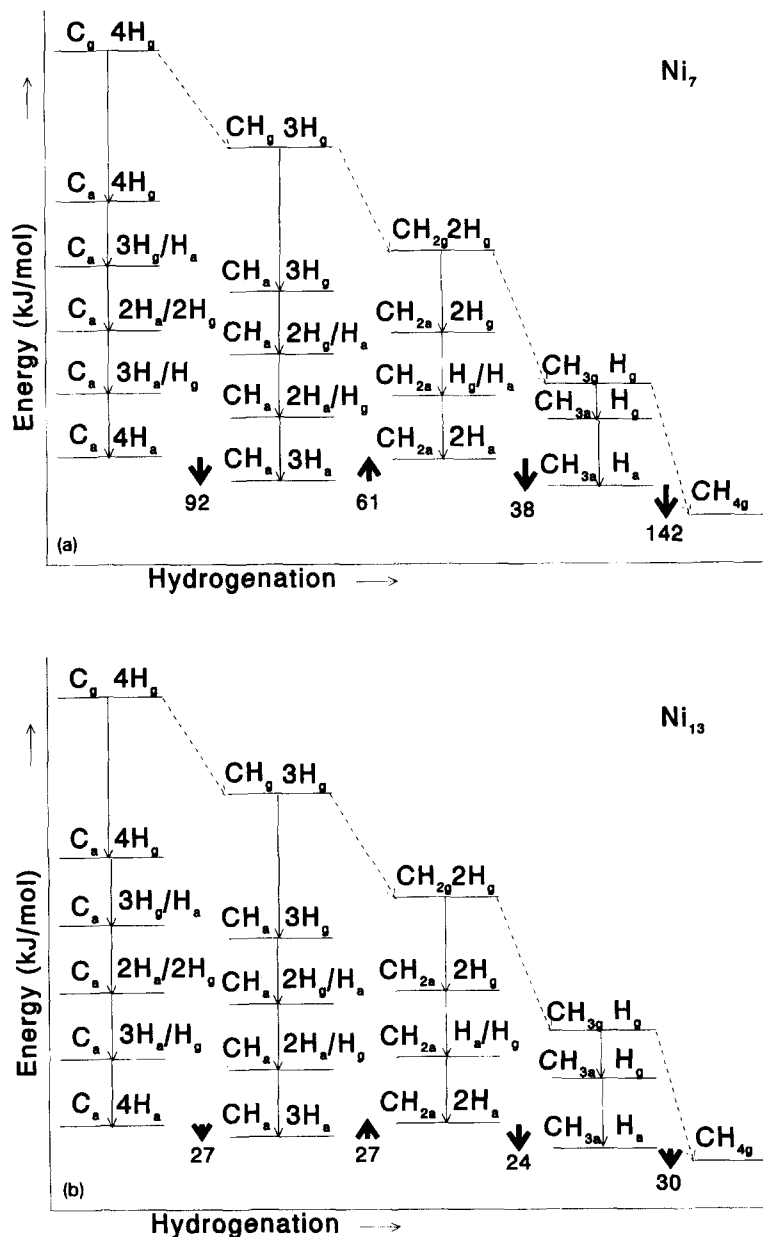


Fig. 2. Energy scheme for CH_4 decomposition and subsequent dehydrogenation to C_a and 4 H_a on Ni_7 (a) and Ni_{13} (b). The adsorption energies of the H and CH_x species used for this scheme are given in Table 2. Geometric and electronic data of these species is discussed in Section 2.

experimental ground state. The barrier to move along the surface, again computed as the difference in chemisorption energy between most preferred site and next-most preferred site, is 49 kJ/mol on Ni₇ and 77 kJ/mol on Ni₁₃. CH prefers the three-fold site on both clusters, but the chemisorption energy of 536 kJ/mol on Ni₇ and 537 kJ/mol on Ni₁₃ are almost the same. The barrier to move along the surface is now 48 kJ/mol on Ni₇ and 100 kJ/mol on Ni₁₃. C also prefers the three-fold site on both clusters, with chemisorption energies of 559 kJ/mol on Ni₇ and 595 kJ/mol on Ni₁₃. The mobility barriers are now 54 kJ/mol on Ni₇ and 119 kJ/mol on Ni₁₃. We thus find the following order in mobility for both nickel clusters:

$$\text{mobility(H)} > \text{mobility(CH}_3) > \text{mobility(CH}_2) \\ > \text{mobility(CH)} > \text{mobility(C)},$$

indicating that H is a very mobile adsorbate whereas C is very immobile.

Siegbahn et al. [13] computed for CH₂ adsorption on Ni(111) modelled by a Ni₃ cluster, an adsorption energy of 324 kJ/mol and estimated it to be 368 kJ/mol. For CH they computed a value of 452 kJ/mol and estimated it to be 502 kJ/mol. They gave no results for C adsorption. Yang and Whitten [15] found for CH₂ a preference for the three-fold site with an adsorption energy of 281 kJ/mol, and an adsorbate–substrate frequency of 430 cm⁻¹. For the two-fold site, they computed an adsorption energy of 262 kJ/mol and an adsorbate–substrate frequency of 444 cm⁻¹. Finally, for the one-fold site they found an adsorption energy of 152 kJ/mol and an adsorbate–substrate frequency of 501 cm⁻¹. Except for the one-fold adsorption energy, which is significantly larger in our case, this is all in good agreement with our data on Ni₇. For CH adsorption they also found a preference for the three-fold site with an adsorption energy of 302 kJ/mol and an adsorbate–substrate frequency of 556 cm⁻¹. For the two-fold site they found an adsorption energy of 280 kJ/mol and an adsorbate–substrate frequency of 447 cm⁻¹. Finally for the one-fold site they found an adsorption energy of 163 kJ/mol and an adsorbate–substrate frequency of 600 cm⁻¹. It is clear from Table 2 that our adsorption energies on the two-fold site and three-fold site are very much higher as are

our adsorbate–substrate stretch frequencies. For the one-fold site the differences are smaller, but still fairly large. Therefore, adsorption energies and adsorbate–substrate frequencies vary strongly on average between Siegbahn et al., Yang and Whitten, and this work, but all groups find the following order in chemisorption energy:

$$E_{\text{ads}}(\text{CH}_3) < E_{\text{ads}}(\text{H}) < E_{\text{ads}}(\text{CH}_2) < E_{\text{ads}}(\text{CH}) \\ < E_{\text{ads}}(\text{C}).$$

The largest difference is found in the case of CH adsorption at the three-fold position on Ni(111), where Siegbahn gives a value of 502 kJ/mol and Yang and Whitten of 302 kJ/mol. A possible reason for these differences has already been discussed in Section 3.1.

The decomposition of CH₄ to C_a and 4H_a is displayed in Figs. 2a and 2b. The first step, activation of one CH bond in gas phase CH₄ producing CH_{3a} and H_a (reaction 1), is 142 kJ/mol endothermic on Ni₇. This is quite large and due to the weak bonding of CH₃ on this cluster. On Ni₁₃ cluster this cluster defect is remedied and the endothermicity drops to 30 kJ/mol. This is quite close to the expected thermoneutrality of the reaction. The second step, abstraction of another hydrogen from CH_{3a} to form CH_{2a} and H_a (reaction 2), is endothermic by 38 kJ/mol on the Ni₇ cluster and 24 kJ/mol on the Ni₁₃ cluster. The third step, decomposition of CH_{2a} to form CH_a and H_a (reaction 3) is exothermic by 61 kJ/mol on Ni₇ and 27 kJ/mol on Ni₁₃, suggesting the thermodynamic instability of this species. This could explain why the group of Ceyer [1] could not find evidence for the existence of CH₂ on a Ni(111) surface, although Kaminsky et al. [2] claim experimental evidence of all CH_x species. Finally, the reaction of CH_a to produce C_a and H_a (reaction 4) is 92 kJ/mol endothermic on Ni₇ and 27 kJ/mol endothermic on Ni₁₃. We conclude that all reaction energies are lowered on the Ni₁₃ cluster compared to the Ni₇ cluster.

Using the experimental CH bond scission energy in CH₄, which is 425 kJ/mol, and the maximum adsorption energies for H and CH₃, which are 259 and 162 kJ/mol, Yang and Whitten computed for reaction 1 an endothermicity of just 4 kJ/mol. For reaction 2 they computed an endothermicity of 55

kJ/mol and for reaction 3 an endothermicity of 140 kJ/mol. Siegbahn et al. found the following reaction energies. For reaction 1, again using the experimental CH bond scission energy in CH₄, the experimental adsorption energy of hydrogen (264 kJ/mol), and their best estimates of the adsorption energy of CH₃ (209–230 kJ/mol [14]), they found an exothermicity of 48–69 kJ/mol. For reaction 2, they computed an endothermicity of 34–58 kJ/mol. For reaction 3 they found an endothermicity of 29 kJ/mol. Finally, for reaction 4 they found an exothermicity of 50 kJ/mol. It seems, that the value they give for reaction 1, i.e. 48–69 kJ/mol exothermic, do not coincide with the reported low sticking coefficients on these surfaces [21]. Only on reaction 2 do all authors agree that it is an endothermic reaction.

3.3. CH₃, CH₂, CH, C and H adsorption on cobalt clusters

In this section we will discuss the chemisorption data for all CH_x species and H on cobalt, which is displayed in Table 3 and Figs. 3a and 3b. For CH₃, we find again a preference for the one-fold site on both Co₇ and Co₁₃. The adsorption energies of 105 and 202 kJ/mol are somewhat higher than on the corresponding nickel clusters. The barrier to move along the surface is 35 kJ/mol on Co₇ and 42 kJ/mol on Co₁₃. CH₂ prefers the three-fold site with adsorption energies of 361 kJ/mol on Co₇ and 397 kJ/mol on Co₁₃. The mobility barrier is 95 kJ/mol on Co₇ and 43 kJ/mol on Co₁₃. CH prefers the three-fold site with adsorption energies of 586 kJ/mol on Co₇ and 564 kJ/mol on Co₁₃. This is the only case in which a fragment adsorbs stronger on a 7-atom cluster than on a 13-atom cluster. The mobility barrier is 258 kJ/mol on Co₇ and 56 kJ/mol on Co₁₃. C prefers the three-fold site with adsorption energies of 625 kJ/mol on Co₇ and 635 kJ/mol on Co₁₃. The mobility barrier is 190 kJ/mol on Co₇ and 86 kJ/mol on Co₁₃. Finally, H also prefers the three-fold site with adsorption energies of 240 and 270 kJ/mol on Co₇ and Co₁₃ and mobility barriers of just 5 and 1 kJ/mol respectively. We thus find the same order in mobility for H and CH_x as we found for the nickel clusters with the exception of CH on Co₇, which is very immobile. It is clear that the site preference for all adsorbates is the same for

Table 3

CH₃, CH₂, CH, C, and H chemisorption on Co₇, and Co₁₃ clusters

Adsorbate	Substrate	Site	<i>z</i> (Å)	<i>E</i> _{ads} (kJ/mol)	<i>ν</i> (cm ⁻¹)
CH ₃ ^a	Co ₇	1-fold	2.09	105	365
CH ₃	Co ₇	2-fold	1.94	70	251
CH ₃	Co ₇	3-fold	1.98	64	245
CH ₃	Co ₁₃	1-fold	2.08	202	556
CH ₃	Co ₁₃	2-fold	1.86	160	234
CH ₃	Co ₁₃	3-fold	1.93	151	284
CH ₂ ^b	Co ₇	1-fold	1.80	266	719
CH ₂	Co ₇	2-fold	1.75	258	260
CH ₂	Co ₇	3-fold	1.37	361	418
CH ₂	Co ₁₃	1-fold	1.79	354	577
CH ₂	Co ₁₃	2-fold	1.53	329	391
CH ₂	Co ₁₃	3-fold	1.48	397	725
CH	Co ₇	1-fold	1.65	328	729
CH	Co ₇	2-fold	1.66	320	689
CH	Co ₇	3-fold	1.20	586	599
CH	Co ₁₃	1-fold	1.66	436	695
CH	Co ₁₃	2-fold	1.40	508	758
CH	Co ₁₃	3-fold	1.29	564	554
C	Co ₇	1-fold	1.64	435	822
C	Co ₇	2-fold	1.60	418	577
C	Co ₇	3-fold	1.03	625	438
C	Co ₁₃	1-fold	1.60	494	683
C	Co ₁₃	2-fold	1.24	549	502
C	Co ₁₃	3-fold	1.09	635	634
H	Co ₇	1-fold	1.48	213	1425
H	Co ₇	2-fold	1.06	235	2094
H	Co ₇	3-fold	0.95	240	1056
H	Co ₁₃	1-fold	1.50	242	1229
H	Co ₁₃	2-fold	1.21	269	1746
H	Co ₁₃	3-fold	1.03	270	1068

Adsorption energies are given relative to the gas phase fragments with the same geometry in their lowest electronic state. For more specific details, see Section 2. *z* denotes the perpendicular adsorbate–substrate distance, *ν* denotes the adsorbate–substrate vibrational stretch frequency.

^a All CH₃ adsorption energies drop 34 kJ/mol if we allow for CH₃ relaxation in the gas phase to adopt the preferred planar CH₃ (²A₂[′]) configuration.

^b All CH₂ adsorption energies drop 25 kJ/mol if we allow for CH₂ relaxation in the gas phase to adopt the preferred CH₂ (³Σ_g⁻) configuration.

nickel and cobalt, i.e. one-fold for CH₃ and three-fold for all other species. The adsorption energies on cobalt are somewhat higher for all CH_x species; for hydrogen they are the same. The same order in chemisorption energy is found on both metals, however the mobility barriers on the 13-atom cluster

have now decreased compared to those on the 7-atom cluster, except for CH_3 , which is just opposite to the results on the nickel clusters. Contrary to nickel, there is no much data available for adsorption on cobalt clusters. However, Zheng et al. [22], using

extended Hückel calculations, gave bonding energies for CH_3 adsorption on slabs modelling $\text{Co}(0001)$ of 360 kJ/mol for the one-fold site, 255 kJ/mol for the two-fold site, and 228 kJ/mol for the three-fold site. We find the same order in site preference on both

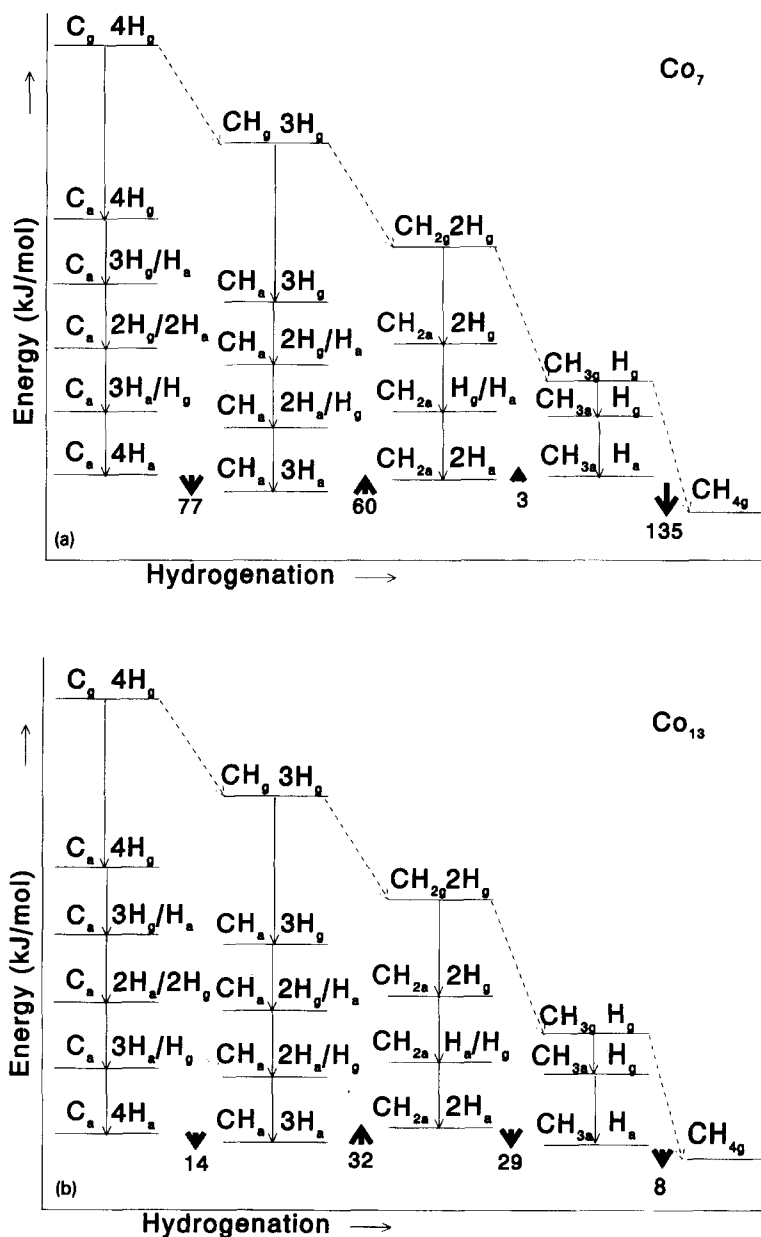


Fig. 3. Energy scheme for CH_4 decomposition and subsequent dehydrogenation to C_2 and 4H_2 on Co_7 (a) and Co_{13} (b). The adsorption energies of the H and CH_x species used for this scheme are given in Table 3. Geometric and electronic data of these species is discussed in Section 2.

Co₇ and Co₁₃ but the energies are much lower. For CH₂ they found a preference for the two-fold site with an adsorption energy of 613 kJ/mol, followed by an adsorption energy of 610 kJ/mol for the one-fold site and 555 kJ/mol for the three-fold site. Again our adsorption energies are much lower, and we find the opposite order for site preference. For CH they calculated a preference for the three-fold site with an adsorption energy of 903 kJ/mol, followed by the two-fold site with an adsorption energy of 873 kJ/mol and the one-fold site with an adsorption energy of 853 kJ/mol. We have the same order for site preference, but again our energies are much lower. All the CH_x species are very mobile on Co(0001) according to Zheng et al.,

The decomposition of CH₄ to C_a and 4H_a is displayed in Figs. 3a and 3b. Reaction 1 is endothermic by 135 kJ/mol on Co₇ and by 8 kJ/mol on Co₁₃. Again this difference is due to a cluster defect, which is remedied in the 13-atom cluster case. Reaction 2 is 3 kJ/mol exothermic on Co₇ and 29 kJ/mol endothermic on Co₁₃. Reaction 3 is exothermic by 60 kJ/mol on Co₇ and 32 kJ/mol on Co₁₃, indicating the thermodynamic instability of the CH₂ species also on cobalt. Finally, reaction 4 is endothermic by 77 kJ/mol on Co₇ and by 14 kJ/mol on Co₁₃. Again all reaction energies are thus lowered on the Co₁₃ cluster compared to the Co₇ cluster. For reaction 2 this effect results in inversion of the energetics from slightly exothermic on Co₇ to endothermic on Co₁₃.

4. Conclusions

We have carried out DFT calculations to study the adsorption of CH₃ and H on nickel clusters of various size and shape. We conclude that a one-layer 7-atom model has at its main advantage that it models a Ni(111), Co(111) and Co(0001) surface. The most important disadvantage is that it suffers from boundary effects. These boundary effects are eliminated by adopting a spherical 13-atom cluster. The main disadvantage is now the transferability of our results on this cluster to those which are experimentally determined on surfaces. As a next step we have studied the adsorption of CH₃, CH₂, CH, C, and H on these clusters.

Starting from gas phase CH₄, the formation of CH_{3a} and H_a is endothermic on all clusters, but the endothermicity is strongly reduced on the 13-atom clusters (142 kJ/mol on Ni₇, 135 kJ/mol on Co₇, 30 kJ/mol on Ni₁₃, and 8 kJ/mol on Co₁₃). The formation of CH_{2a} and H_a from CH_{3a} is endothermic by 25–40 kJ/mol on all clusters, except on Co₇ (3 kJ/mol exothermic), mainly because of the much stronger adsorption of CH₂ on this cluster. The formation of CH_a and H_a from CH_{2a} is exothermic on all clusters, but the exothermicity differs a factor two between the 7- and 13-atom clusters (61 kJ/mol on Ni₇, 60 kJ/mol on Co₇, 27 kJ/mol on Ni₁₃, and 32 kJ/mol on Co₁₃). Finally, the formation of C_a and H_a from CH_a is strongly endothermic on the 7-atom clusters, but the endothermicity is again strongly reduced on the 13-atom clusters (92 kJ/mol on Ni₇, 77 kJ/mol on Co₇, 27 kJ/mol on Ni₁₃, and 14 kJ/mol on Co₁₃).

All authors agree on reaction 2 being endothermic. We found reaction 3 to be exothermic. This is in line with the observation of Ceyer's group [1] of CH₃ and CH but not of CH₂. Furthermore, we find all species to adsorb at three-fold sites except for CH₃, which adsorbs at a one-fold site. Zheng et al., using extended Hückel calculations, agree with us on this last point, as they found that all species wanted to restore their missing bonds. They disagree with us and the groups of Siegbahn and Whitten on the point of adsorption site of the other species. Our computed CH₃ chemisorption energies seem too low on the 7-atom clusters, but this is remedied at the 13-atom clusters. It seems that Siegbahn et al. overestimate the CH₃ adsorption energy, because they report for reaction 1 an endothermicity of 48–69 kJ/mol, which does not coincide with the reported low sticking coefficients. No CH_x adsorption energies are known experimentally. The large differences between the calculated results remains controversial, but a possible origin is the different treatment of the nickel valence d orbitals among the groups.

Acknowledgments

All calculations were performed with the ADF program on the Cray Y-MP4/464 at SARA, Amsterdam. This work has been supported by the Nether-

lands Foundation for Chemical Research (SON) with financial aid from the Netherlands Organization of Pure and Scientific Research (NWO). The computer time on the Cray Y-MP4/464 was subsidized by the Foundation for the use of supercomputers, National Computing Facilities (NCF).

References

- [1] M.B. Lee, Q.Y. Yang and S.T. Ceyer, *J. Chem. Phys.* 87 (1987) 2724.
- [2] M.P. Kaminsky, N. Winograd, G.L. Geoffroy and M.A. Vannice, *J. Am. Chem. Soc.* 108 (1986) 1315.
- [3] Amsterdam density functional (ADF) program developed by Baerends and co-workers;
E.J. Baerends, D.E. Ellis and P. Ros, *Chem. Phys.* 2 (1988) 41;
P.M. Boerrigter, G. te Velde and E.J. Baerends, *Int. J. Quantum Chem.* 33 (1988) 87;
G. te Velde and E.J. Baerends, *J. Comput. Phys.* 99 (1992) 84;
D. Post and E.J. Baerends, *J. Chem. Phys.* 78 (1983) 5663;
E.J. Baerends and A. Rozendaal, *Quantum Chemistry: the Challenge of Transition Metals and Coordination Chemistry*, Ed. A. Veillard (Reidel, Dordrecht, 1986);
P.J. van den Hoek, A.W. Kleyn and E.J. Baerends, *Comput. At. Mol. Phys.* 23 (1989) 93.
- [4] D.M. Ceperley and B.J. Alder, *Phys. Rev. Lett.* 45 (1980) 566.
- [5] S.H. Vosko, L. Wilk and M. Nusair, *Can. J. Phys.* 58 (1980) 1200;
J.P. Perdew and A. Zunger, *Phys. Rev. B* 23 (1981) 5048.
- [6] A.D. Becke, *Int. J. Quantum Chem.* 27 (1985) 585.
- [7] A.D. Becke, *Phys. Rev. A* 38 (1988) 3098.
- [8] H. Stoll, C.M.E. Pavlidou and H. Preuss, *Theor. Chim. Acta* 49 (1978) 143;
H. Stoll, E. Golka and H. Preuss, *Theor. Chim. Acta* 55 (1980) 29.
- [9] J.G. Snijders and E.J. Baerends, *Mol. Phys.* 36 (1978) 1789;
J.G. Snijders, E.J. Baerends and P. Ros, *Mol. Phys.* 38 (1979) 1909.
- [10] N. Rösch, L. Ackermann and G. Pacchioni, *Chem. Phys. Lett.* 199 (1992) 275.
- [11] O. Kühnholz and M. Grodzicki, *Lecture Notes in Phys.* 269 (1987) 198.
- [12] T. Ziegler and A. Rauk, *Theor. Chim. Acta* 46 (1977) 1.
- [13] P.E.M. Siegbahn and I. Panas, *Surf. Sci.* 240 (1990) 37.
- [14] J. Schüle, P.E.M. Siegbahn and U. Wahlgren, *J. Chem. Phys.* 89 (1988) 6982.
- [15] H. Yang and Y.L. Whitten, *Surf. Sci.* 255 (1991) 193.
- [16] I. Panas, J. Schüle, P.E.M. Siegbahn and U. Wahlgren, *Chem. Phys. Lett.* 149 (1988) 265;
I. Panas, P.E.M. Siegbahn and U. Wahlgren, *The Challenge of d and f Electrons. Theory and Computation*, Eds. D.R. Salahub and M.C. Zerner (Am. Chem. Soc. Washington, DC, 1989).
- [17] K. Christmann, R.J. Behm, G. Ertl, M.A. Van Hove and W.H. Weinberg, *J. Chem. Phys.* 70 (1979) 4168.
- [18] K. Christmann, O. Schober, G. Ertl and M. Neumann, *J. Chem. Phys.* 60 (1974) 4528.
- [19] W. Ho, N.J. DiNardo and D.E. Plummer, *J. Vac. Sci. Technol.* 17 (1980) 314.
- [20] C.F. Melius, T.H. Upton and W.A. Goddard III, *Solid State Commun.* 28 (1978) 501;
O. Gropen and I. Almlöf, *Chem. Phys. Lett.* 191 (1992) 306;
M.A. Nygren, P.E.M. Siegbahn, U. Wahlgren and H. Akeby, *J. Phys. Chem.* 96 (1992) 3633.
- [21] T.P. Beebe, D.W. Goodman, B.D. Kay and J.T. Yates, Jr., *J. Chem. Phys.* 87 (1987) 2305.
- [22] C. Zheng, Y. Apeloig and R. Hoffmann, *J. Am. Chem. Soc.* 110 (1988) 749.